



Thin-film-composite hollow fiber membranes containing amino acid salts as mobile carriers for CO₂ separation



Zhongde Dai, Jing Deng, Luca Ansaloni, Saravanan Janakiram, Liyuan Deng*

Department of Chemical Engineering, Norwegian University of Science and Technology Trondheim, 7491, Norway

ARTICLE INFO

Keywords:

Hollow fiber membrane
CO₂ separation
Facilitated transport
Mobile carrier
Amino acid salts

ABSTRACT

In this work, defect-free thin-film-composite (TFC) hollow fiber membranes containing various amino acid salts as CO₂ facilitated transport carriers were fabricated via dip-coating. Four different amino acid salts, i.e., potassium proline (ProK), potassium arginine (ArgK), potassium glycinate (GlyK) and potassium cysteine (CysK), were selected and embedded within polyvinyl alcohol (PVA) matrix. TGA, FTIR, SEM and humid mixed gas permeation test were used for the evaluation. Experiments show that adding amino acid salts into the PVA matrix significantly increases the CO₂ permeance with little influence on the CO₂/N₂ selectivity. ProK was found the most effective within the four investigated mobile carriers; The addition of 40% ProK into the PVA matrix nearly doubled the CO₂ permeance (from 399 to 791 GPU). The PVA/amino acid salt membranes also exhibited good long-term stability, in which both CO₂ permeance and CO₂/N₂ selectivity remained nearly unchanged in a 20-h test and after a two-week shutdown period.

1. Introduction

Membrane separation is widely accepted as a promising alternative to traditional CO₂ separation technologies (i.e., amine-based absorption and solid adsorption) due to its high modularity, small footprint, low or no chemical emissions and easiness of operation. However, for gas separation, most polymeric membranes follow the solution-diffusion mechanism, thus are subject to a trade-off between the gas permeability and selectivity, which is also known as the performance limitation called “Robeson Upper Bound” [1]. This limitation makes the CO₂ separation membranes not economically favorable in industrial applications [2]. Facilitated transport membranes have been considered an effective solution to overcome this limitation in CO₂ separation processes. Facilitated transport membranes involve the use of carriers that interact specifically and reversibly with the reactive species in the feed gas mixture, which can improve the permeation of the more reactive gases while maintaining or even increasing the selectivity of these gases over other less reactive gases [3,4].

Various carriers have been employed to enhance the CO₂ permeation by the facilitated transport mechanism. The firstly reported facilitated transport membranes are supported liquid membranes (SLMs) containing mobile carriers dissolved in the liquid phase [5]. However, due to the lack of stability, polymeric membranes consisting of CO₂ reactive functional groups (e.g., amino groups) as fixed-carriers,

commonly known as fixed-site-carrier (FSC) membranes, have been reported with excellent stability but compromised CO₂ separation performance [6–11]. The main drawback of the FSC membranes is the low mobility of the carriers and thus the lower CO₂ permeability compared with the membranes containing mobile carriers. Recently, a new approach to stabilizing mobile carriers has been reported in the fabrication of CO₂ facilitated transport membranes, where polymeric matrix is used to host mobile carriers (e.g., task-specific ionic liquids, amino acid salts, and enzymes) and water vapor is usually introduced to swell the membrane matrix and thus improve the mobility of the carriers [7,12,13].

Amines, alkalines, amino acid salts and carbonic anhydrase (CA) have been mostly reported as mobile carriers in CO₂ facilitated transport membranes, while among them the mobile carriers of basic primary amine group (–NH₂) are the most intensively studied [14,15]. However, most of these mobile carriers based facilitated transport membranes were fabricated as self-supported flat sheet membranes or coated onto a flat sheet membrane substrate by either knife casting or dip-coating methods. Hollow fiber facilitated transport membranes and modules have been rarely reported [16,17]. To fabricate hollow fiber thin-film-composite (TFC) facilitated transport membranes is an important step forward to bring this technology from lab to industrial applications, as the intrinsic advantages come from hollow fiber membranes (e.g., high productivity per unit volume, self-supporting

* Corresponding author.

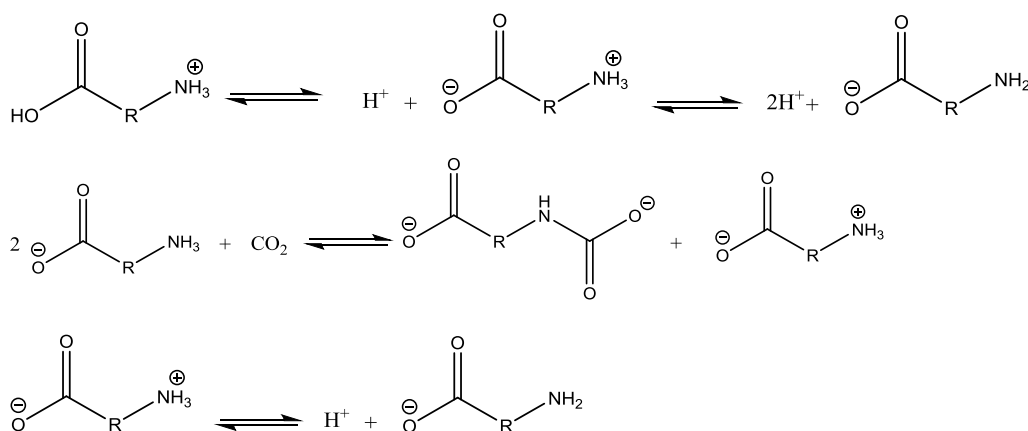
E-mail address: liyuan.deng@ntnu.no (L. Deng).

<https://doi.org/10.1016/j.memsci.2019.02.023>

Received 15 November 2018; Received in revised form 18 January 2019; Accepted 10 February 2019

Available online 13 February 2019

0376-7388/ © 2019 Elsevier B.V. All rights reserved.



Scheme 1. Amino acid salt protonation in water and reaction with CO₂ [20].

without spacer) are essential properties for industrial scale membrane processes.

Compared to the primary amine-based carriers, amino acid salts hold many advantages, including good diffusivity and negligible volatility. Furthermore, membranes containing amino acid salts also exhibit much better stability as the performances are not deteriorated in the presence of oxygen [18].

It is commonly accepted that amino acids in water are in the form of zwitterions with all the amino groups completely protonated [19]. With the presence of water, amino acid salts react with CO₂ following the zwitterionic mechanism similar to its interaction with primary and secondary amines, as shown in Scheme 1:

Due to the fast reaction kinetics and high CO₂ absorption capacity, amino acid salts have been intensively studied as CO₂ absorbents in different absorption processes, including membrane contactors [21]. In recent years, amino acid salts have been used as mobile carriers for CO₂/H₂ and CO₂/N₂ separation in facilitated transport membranes [22]. By blending about 30 wt% of sodium arginate into chitosan matrix, a CO₂ permeability of ~1500 Barrer with the CO₂/N₂ selectivity of 852 and CO₂/H₂ selectivity of 144 was obtained even at a low relative humidity (< 20%) [23]. Amino acid salts were also mixed into SPEEK to improve the CO₂ separation performances [24]. By adding 20% of sodium lysinate, sodium histidinate, and sodium arginate into SPEEK matrix, both CO₂ permeability and CO₂/CH₄ selectivity were improved. Please note that the above-mentioned membranes are self-standing membranes with a thickness of ~60 μm.

Recently, Ho and coworkers reported a membrane using amino acid salts as mobile carriers for CO₂ separation, in which superior CO₂ separation performances (P_{CO₂} > 6000 Barrer and CO₂/N₂ selectivity > 500) was obtained under an optimal operating condition at an elevated temperature of ~107 °C [25]. However, these membranes normally have a thickness of 30–60 μm. Despite the high permeability, the overall gas permeance is in the range of 100–200 GPU, which is much lower than the benchmark set by the Polaris membrane (CO₂ permeance > 1000 GPU). In another report by the same group, three glycine-based amino acid salts were blended with PVAm and fabricated as a flat sheet TFC membrane using polyethersulfone (PESf) substrate [12]. CO₂ permeance of ~1100 GPU with the CO₂/N₂ selectivity over 200 was obtained. Nevertheless, as an additional inorganic zeolite Y seed layer must be employed to reduce the possible solution penetration in this membrane, the membrane fabrication process was somewhat complicated.

In the present work, four different amino acid salts, namely potassium arginate (ArgK), potassium glycinate (GlyK), potassium proline (ProK) and potassium cystinate (CysK), were used as mobile carrier to facilitate the CO₂ transport in membranes based on literature study; Arginine and glycine were reported with high CO₂ separation

performances in membranes [12,23], and Proline has high solubility in water and high CO₂ absorption rate in aqueous solutions [26]. Cystine was used to make comparison to other three amino acids. Poly(vinyl alcohol) (PVA), a cheap and biodegradable polymer, was employed as the polymer matrix to host the amino acid salt mobile carriers. PPO (Poly (*p*-phenylene oxide)) hollow fibers were used as the support substrates to fabricate the TFC membranes. The resultant TFC hollow fiber membranes with a selective layer thickness of smaller than 500 nm were tested in a humid mixed gas permeation rig. The CO₂ separation performance of the resultant membrane was investigated using the CO₂/N₂ gas mixture as feed gas at 100% relative humidity (RH) and room temperature. The thermal stability and chemical structure of the membrane materials and morphology of the TFC membranes were characterized using TGA, FTIR, and SEM, respectively. The stability of the membrane performance was evaluated through a 20-h continuous test and by comparing the performances before and after a shut-down operation for two weeks.

2. Experimental

2.1. Materials

Poly(*p*-phenylene oxide) (PPO) hollow fiber membrane was kindly supplied by Parker, Norway. Poly(vinyl alcohol) (PVA, Mn 7.9 k ~ 12 k, 89% hydrolyzed), glycine (98.5%), L-proline (> 99%), L-cysteine (> 97%), L-arginine (> 98%), and potassium hydroxide (KOH, reagent grade) were ordered from Sigma, Germany. All chemicals were used as received without further purification. The chemical structures of the four amino acids are shown in Fig. 1.

2.2. Membrane and membrane module preparation

All amino acid salts were synthesized by mixing the stoichiometric amount of amino acids with KOH in DI water (10 wt%), while the 4 wt % PVA solution was prepared by dissolving PVA in water at 80 °C for 4 h under reflux. The desired amounts of the amino acid salts and PVA solution were then mixed at different weight ratios. The total solid (PVA + amino acid salts) concentration in the coating solution was diluted to 0.5 wt% in water. The PVA/amino acid salt solution was filtrated using a 0.65 PTFE filter membrane prior to each membrane coating process.

The amino acid salts content (ω_{AAS} , wt%) in each hybrid membrane was calculated from equation (1):

$$\omega_{AAS} = \frac{w_{AAS}}{w_{AAS} + w_{PVA}} \times 100 \quad (1)$$

where w_{AAS} and w_{PVA} are the weights of amino acid salt and PVA,

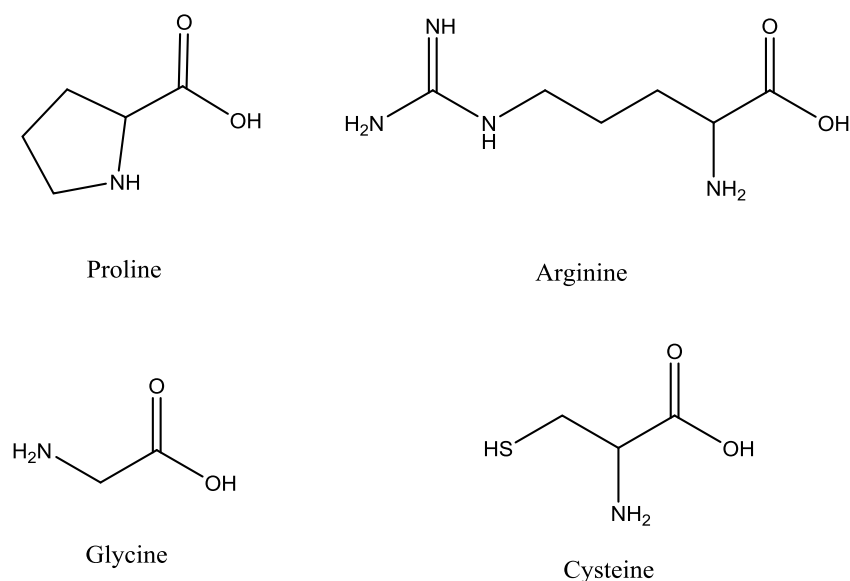


Fig. 1. Chemical structure of the four selected amino acid salts.

respectively.

Afterward, the mixed solution was dip-coated onto a PPO hollow fiber substrate following an optimized procedure (as shown in Scheme S1 in supporting information). First, the PPO hollow fibers were gently washed with DI water for a few minutes to remove the dust from the surface before coating. The PPO hollow fibers were then dipped into the coating solution for 10 s, vertically withdrawn from the solution, and hung in the air for about 6 h before the second coating. The coated membranes were turned up-side-down and dip-coated again following the same procedure to eliminate defects, and the membranes were hung in the air for another 6 h after the second coating. These steps are at ambient condition. Finally, the coated fibers were dried in a vacuum oven at 60 °C for at least 6 h before further characterization.

The hollow fiber membrane module was fabricated by putting 10 hollow fibers in a 3/8 inch Swagelok™ stainless tube (As shown in Fig. 2). The effective length of the HF membrane is 10 cm. Epoxy glue used to seal the membrane was Aradite™ 2020 purchased from Lindberg-lund, Norway.

2.3. Membrane characterization

The thermal stability of the PVA and the amino acid salts were studied using a thermal gravimetric analyzer (TGA, TG 209F1 Libra, Netzsch, Germany). The temperature was in the range from room

temperature to 700 °C with the increasing rate of 10 °C/min. N₂ was used as both purge gas (20 mL/min) and protection gas (20 mL/min) during the test. For the characterization, the dried amino acid salts were prepared by drying the solution using rotary evaporator at 40 °C. The obtained amino acid salts are white or slightly yellowish powder.

Membrane morphology was studied using a scanning electron microscope (SEM, TM3030 tabletop microscope, Hitachi High Technologies America, Inc.). Cross-section samples were prepared by breaking the hollow fibers in liquid N₂. In order to ensure good electrical conductivity on the surface, all the samples were coated with gold for 2 min with a sputter coater.

FTIR spectra of the samples were obtained from a Thermo Nicolet Nexus spectrometer with a smart endurance reflection cell (Golden Gate high performance single reflection monolithic diamond ATR). Spectrums were averaged over 16 scans at a wavenumber resolution of 4 cm⁻¹ in the range of 650 cm⁻¹ to 4000 cm⁻¹.

Gas separation performance was measured in the home-made mixed gas permeation test setup with humidifiers to control the relative humidity of the feed and permeate gas streams [27,28]. A 10/90 v/v% CO₂/N₂ gas mixture was used as the feed gas, whereas pure CH₄ was used as the sweep gas. The feed pressure was held at 2 bar while the sweep side pressure was kept at 1.05 bar for all the experiments. The compositions of retentate and permeate streams exiting the membrane module were monitored by a calibrated gas chromatograph (490 Micro

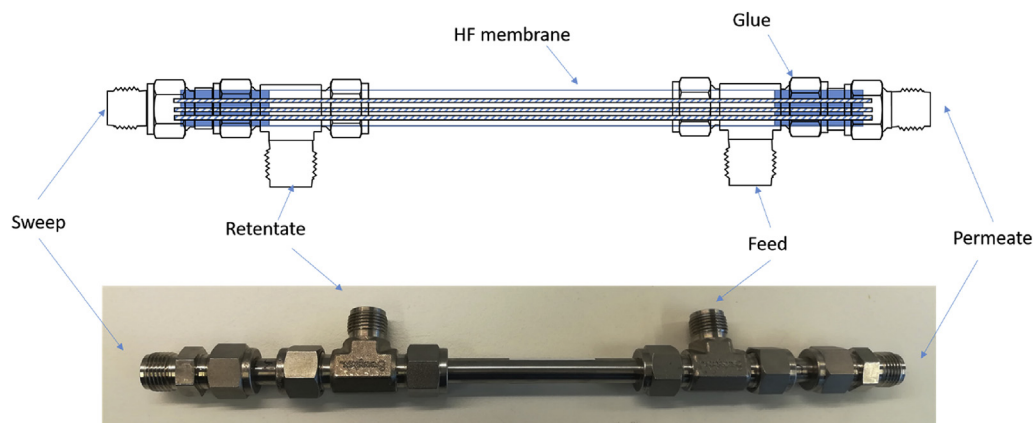


Fig. 2. Hollow fiber membrane module used in the present study.

GC, Agilent) throughout the test. Two columns were used in the GC to analyze the gas composition (a 20 m MS5A, and a 10 m PPQ). Each test continued for at least 10 h to ensure the steady state. Due to the difficulties of obtaining the actual selective layer thickness of a swollen membrane in a humid gas stream and the undefined transport resistance of the porous substrates, the permeation properties of the membrane were only reported as gas permeances, not permeability.

The permeance (P_i) of the i th penetrant species was measured by

$$P_{m,i} = \frac{N_{perm}(1 - y_{H_2O})y_i}{A(p_{i,feed} \cdot p_{i,ret} - p_{i,perm})} \quad (2)$$

where N_{perm} is the total permeate flow measured with a bubble flow meter, y_{H_2O} is the molar fraction of water in the permeate flow (calculated according to the RH value and the vapor pressure at the given temperature), y_i is the molar fraction of the species of interest in the permeate, and $p_{i,feed}$, $p_{i,ret}$ and $p_{i,perm}$ identify the partial pressures of the i th species in the feed, retentate and permeate, respectively. The separation factor ($\alpha_{ij} = \frac{y_i/x_i}{y_j/x_j}$) was applied for mixed-gas permeation tests. All the gas permeation data reported in the current work were obtained from at least two membrane samples with a deviation lower than 10%, and thus the error bar was not presented.

3. Results and discussion

3.1. Thermal properties

TGA analysis was used to conduct the thermal stability test of the resulted membranes. One distinct advantage of amino acids compared to other amine-based mobile carriers is the low vapor pressure and good thermal stability. Based on a recent report [29], most of the amino acids exhibit a T_{onset} higher than 200 °C. T_{onset} is the temperature at the onset of thermal degradation, determined in the TGA graph by the intersection of the baseline weight and the tangent of the weight dependence on the temperature curve as decomposition occurs [30]. In this study, GlyK and ProK show quite similar TGA curve in the first stage, which have a T_{onset} of ~220 °C (as shown in Fig. 3(A)). On the other hand, even though arginine and cysteine have been reported to have the T_{onset} of 236 and 245 °C, respectively, the ArgK and CysK presented lower T_{onset} values compared to their acid forms. A T_{onset} of ~130 for ArgK and 150 °C for CysK were obtained. It has been reported that the thermal stability has a trend following the order of diamine > alkanolamine > amino acid salt [31] and that amino acids with primary amines degrade faster than those containing secondary amines. As expected, in this work, ProK also shows much better thermal stability due to the secondary amine functional groups, while CysK (containing -SH function groups) and ArgK (with multi-primary amine groups) exhibit relatively lower thermal stability.

Amino acid salts were reported to mainly undergo amide formation at high temperature stripping conditions, during which the amine

groups function as a nucleophile to intermolecular attack [32]. Moreover, it is clearly shown that at a higher temperature (> 450 °C), GlyK shows a higher residual mass compared to other amino acid salts, probably due to the higher possibility of forming cross-linked structure from the primary amine group in glycine. Other three amino acid salts show similar residual mass.

The TGA curves of PVA/GlyK hybrid membranes with different GlyK content are presented in Fig. 3(B). As can be seen, T_{onset} of the hybrid membranes decreases with the increasing GlyK content in the hybrid membranes. Moreover, different from the PVA membrane, the PVA/GlyK hybrid membranes exhibit a three-stage decomposition curve. By comparing Fig. 3 (A) and 3(B), it is clear that the first stage mainly comes from the decomposition of GlyK. However, the primary amine groups from Glycine become more reactive at higher temperatures, forming a cross-linked structure in the membrane with better thermal stability, and hence showing the second stage decomposition. Moreover, with increasing GlyK content, the first stage weight loss decreases while the mass retention at $T > 450$ °C increases, possibly due to that at high temperature ($T > 450$ °C), the inactions between GlyK and PVA became stronger and resulted in a more stable cross-linked structure. Other three amino acid salts show similar TGA curves compared to PVA/GlyK, as presented in the supporting information (Figs. S1–S3).

According to the TGA analysis, the PVA/amino acid salt hybrid membranes have a high thermal stability that fulfills the requirements for common CO₂ separation processes, including CO₂ capture from post-combustion flue gas.

3.2. FTIR analysis

FTIR analysis was employed to investigate the interaction between PVA and different amino acid salts, as shown in Fig. 4.

As it can be seen from Fig. 4 (A), a broad peak can be observed for all the four tested amino acid salts in the higher energy region between 3100 cm⁻¹ and 2600 cm⁻¹, which is assigned to the NH₃⁺ stretching vibrations, where the two relatively higher double peaks at ~2990 cm⁻¹ may be assigned to C–H₂ asymmetric stretching or N–H asymmetric stretching. The NH₃⁺ stretching region also shows broad band characteristic of hydrogen bonding. Considering CysK, due to the -SH group, three characteristic peaks can be found at 2370 cm⁻¹, 1140 cm⁻¹, and 944 cm⁻¹, corresponding to -SH stretching, S=O stretching and -SH bending, respectively [33]. Similar characteristic peaks can also be found for ArgK, which is at 1680 cm⁻¹ and can be assigned to the -NH₂ and =NH groups [34]. In the range of 1560–1400 cm⁻¹, two prominent peaks can be observed for all the four samples, which can be assigned to the -COO asymmetric stretching, -COO symmetric stretching, and CH₂-CO deformation, respectively. Peaks appearing in a lower wavelength range are mainly due to C–H, C–N or C–C stretching. Detailed assignments can be found in Table 1.

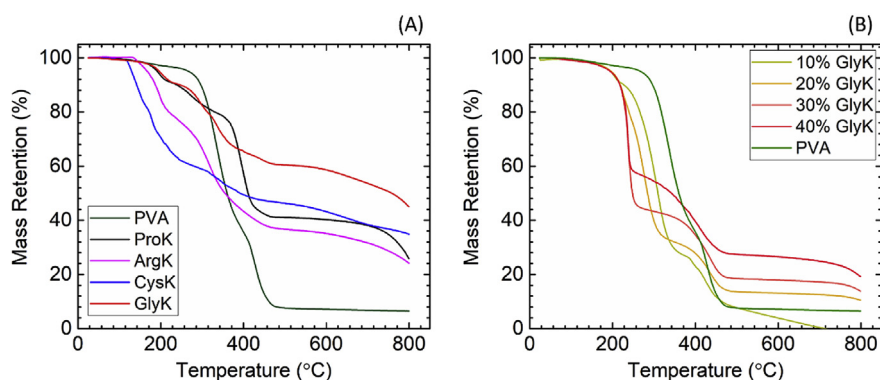


Fig. 3. Thermal properties of various amino acid salts and PVA (A), and PVA/GlyK hybrid membranes with different contents of GlyK (B).

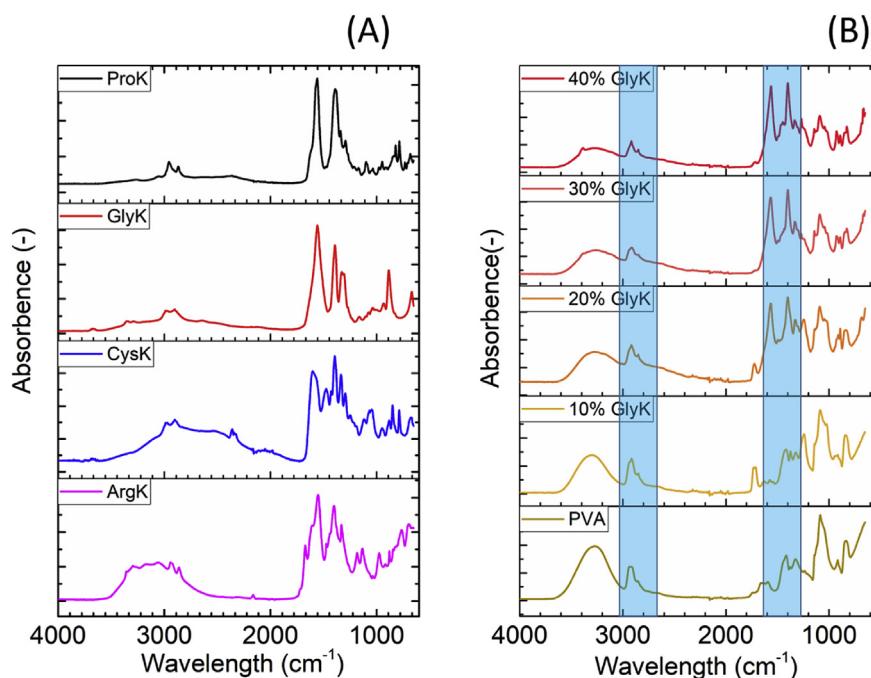


Fig. 4. FTIR spectrum of PVA and four different amino acid salts.

Table 1

Peak assignments of PVA and four different amino acid salts.

Peak position (cm ⁻¹)				Peak assignment
GlyK	ProK	CysK	ArgK	
3431			3150	N–H asymmetric stretching
2990	2960	2910	2928	C–H ₂ asymmetric stretching, N–H asymmetric stretching
2609	2880			N–H–O stretch
		2370		SH stretching
			1680	NH ₂ bending
1560	1570	1645	1560	–COO asymmetric stretching
		1432		CH bending
			1461	CH ₃
1404	1400		1400	–COO symmetric stretching, CH ₂ –CO deformation
		1346		NH ₃ bending, symmetric
1332	1330		1330	C–H stretching
	1292	1292		C–H ₂ wagging
			1190	C–C–C symmetric stretching
1124	1168		1130	C–N stretching
		1140		S=O stretching
1038	1051	1063		C–N stretching
		944		SH bending
924	928			C–C stretching
889			896	C–C stretching, NH ₃ rocking
		815		COO wagging
		776	794	C–C stretching, NH ₃ rocking

As clearly shown in Fig. 4(B), many characteristic peaks of GlyK can be found in the hybrid membranes. The two peaks at 2900 and 2660 are attributed to NH₃⁺ stretching vibrations, and two peaks in the range of 1560–1400 cm⁻¹ are due to the –COO asymmetric stretching and –COO symmetric stretching. The intensity of these characteristic peaks is proportional to the GlyK content in the hybrid membranes.

FTIR analysis confirms the chemical structures of the selected amino acid salts. In addition, as no new peaks or peak shift can be found for all the samples, it is clear that there is no chemical interaction between GlyK and PVA in the hybrid membranes under the test conditions.

3.3. Membrane coating procedure and morphology study

It is well-known that different parameters such as the coating solution concentration, dipping times/duration as well as the dipping rate, have significant effects on the final membrane morphology and thickness, and consequently, the overall separation performances. In the current work, dip-coating was done manually. Although the dipping rate cannot be controlled quantitatively, the dipping time and coating solution concentration were optimized through repeated trial-and-errors. As the PPO hollow fiber substrate has a dense surface, there is no need to worry about the pore penetration problem, and it is found that changing the dipping duration from 10 s to 30 s did not have significant effect on the overall thickness, thus 10 s were used. Three coating solution concentrations had been studied, i.e., 0.25 wt%, 0.5 wt% and 1 wt%. The membrane fabricated via 0.25 wt% coating solution had relatively lower CO₂/N₂ selectivity, which was close to the neat PPO support, demonstrating that the PPO substrate was not fully covered by the PVA layer. The membrane fabricated via 1.0 wt% coating solution resulted in a much thicker selective layer with CO₂ permeance lower than 200 GPU, thus 0.5 wt% was selected as the optimized concentration for membrane coating.

The membrane morphology and coating layer thickness were investigated using SEM, as shown in Fig. 5, the overall membrane cross-section morphology (left) and the coating layer (right). According to the SEM images obtained from different parts of the coated hollow fiber membranes, a layer with a thickness of around 500 nm has been evenly coated onto the hollow fiber PPO substrate. From the SEM images of more membranes containing various amounts of amino acid salts (as shown in Fig. S4 in supporting information), it is also found that increasing amino acid salt content in the membrane has a negligible effect on the selective layer thickness. The viscosity of the coating solution is one of the most dominating effects on the coating layer thickness [35]. In the current study, the low polymer concentration in the coating solution (0.5 wt%) has resulted in a very low overall viscosity, while adding amino acid salts into solutions at such a low concentration does not significantly change the viscosity value; thus a quite similar coating layer thickness has been obtained in the membranes.

Membranes with other three amino acid salts were also studied using SEM. The TFC membranes with similar selective layer thickness

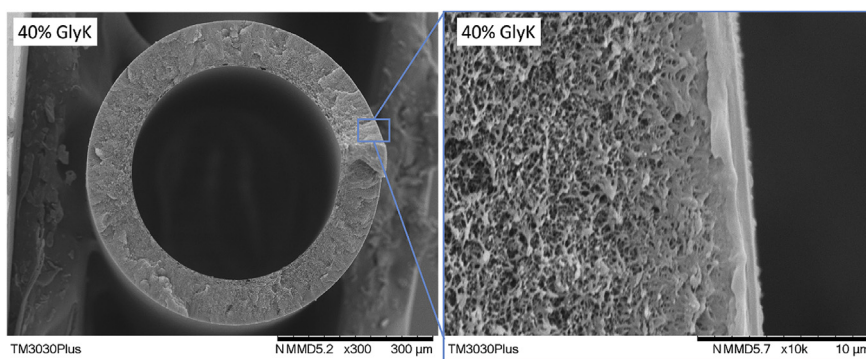


Fig. 5. Membrane morphology of PVA/GlyK membrane with 40 wt% GlyK.

were obtained, as shown in Fig. S5 ~ S7. It is evident that membranes with 40 wt% GlyK, 40 wt% ProK, 40 wt% CysK and 30 wt% ArgK all present a thickness of around 500 nm or lower.

3.4. Mixed-gas permeation studies

The CO₂ separation performances of the PVA/amino acid salt membranes were investigated using CO₂/N₂ (10/90 vol%) mixed feed gas at 100% relative humidity and room temperature. Fig. 6(A) shows the CO₂ permeance as a function of amino acid salt content in the hybrid membranes. For neat PVA membrane fabricated with 0.5 wt% PVA solution, a CO₂ permeance of 399 GPU is obtained. Adding the amino acid salts into the PVA matrix significantly improves CO₂ permeance of the hybrid membranes.

In the case of ProK, the CO₂ permeance increases with ProK content in the membrane: at 40 wt% of ProK, CO₂ permeance of 791 GPU is obtained, which is almost doubled compared to the neat PVA membrane. This value is the highest obtained among the four hybrid membranes consisting of different amino acid salts. A similar trend is observed for the ArgK membrane. Increasing ArgK content to 30 wt% in the hybrid membrane results in CO₂ permeance of 660 GPU, which is 1.65 times of the pristine PVA membrane permeance. Attempts were made to increase the ArgK content further in the membrane. However, at a higher ArgK concentration, precipitations was observed in the PVA-ArgK solution, and no defect-free membrane coating was obtained.

Different from the ProK and ArgK membranes where CO₂ permeance increases linearly with amino acid salt content in the membranes, both GlyK and CysK based hybrid membranes show an optimal CO₂ permeances below the highest amino acid salt contents, at 30 wt%. Further increasing the amino acid salt in the membrane leads to a sharp decrease in the separation performances. For instance, the membrane with 30 wt% GlyK gives CO₂ permeance of 616 GPU, but CO₂ permeance of 563 GPU is obtained for the membrane with 40 wt% GlyK. In addition, PVA solution with 40 wt% GlyK and CysK were less stable

compared to PVA/ProK solution with the same amino acid salt concentration. Even though precipitant was not immediately observed in the PVA/amino acid salt solution, a higher GlyK or CysK content in the mixture may lead to micelle formation/aggregation and cause negative impacts on the membrane performances. White flocculation in the mixture was found on the second or third day after the solution was prepared.

CO₂/N₂ selectivity was also investigated, as presented in Fig. 6(B). In this study, the CO₂/N₂ selectivity does not have significant change with the amino acid salts content in the hybrid membranes. Neat PVA membrane exhibits a CO₂/N₂ selectivity of 35.2, while PVA membranes with amino acid salts show CO₂/N₂ selectivity in the range of 35–40. A similar trend has been reported by Chen et al. [12], where an increment of CO₂ permeance from ~700 GPU to ~900 GPU was obtained by increasing GlyK content from 50 wt% to 65 wt% with nearly constant CO₂/N₂ selectivity. The CO₂/N₂ selectivity reported in Ref. [12] is much higher (~170) due to the additional CO₂ facilitated transport carriers (primary amino groups) in the polymeric matrix of polyvinylamine (PVAm), which is in good agreement with our prior work using a PVAm membrane, where CO₂/N₂ selectivity of ~170 at 90% relative humidity has been reported [36]. In another report, sodium glycinate (GlyNa) was blended with Pebax™ 1657 to make membranes for CO₂ separation [37]. Compared with the neat Pebax, the membrane of Pebax with 20 wt% GlyNa exhibited an enhancement of CO₂ permeability from ~300 Barrers to ~1100 Barrers, while both the CO₂/CH₄ selectivity (~30) and CO₂/N₂ selectivity (~50) were almost unaffected.

The CO₂/N₂ selectivity of the membranes in the present study showed similar trends as the literature, in which the presence of amino acid salts in the polymeric phase greatly improved the CO₂ permeance, while the CO₂/N₂ selectivity were only moderately affected. This is a clear indication that the amino acid salts in the membrane not only significantly improve the CO₂ affinity of the membranes and thus promote the CO₂ transport, but also to an extent increase the gas

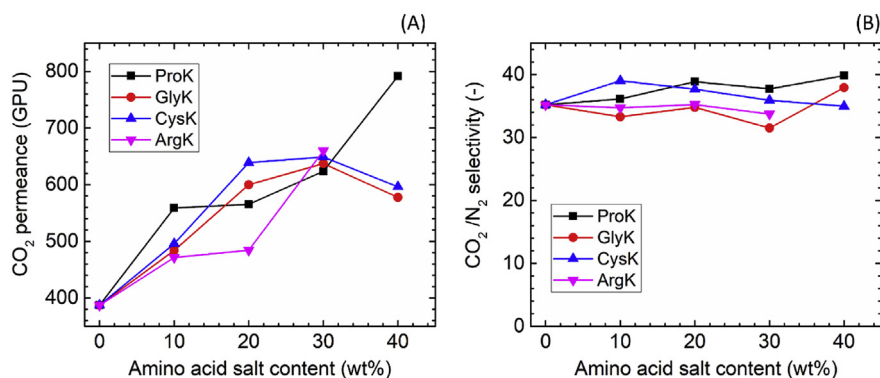


Fig. 6. CO₂ permeance (A) and CO₂/N₂ selectivity (B) as a function of amino acid salts content in the hybrid membranes.

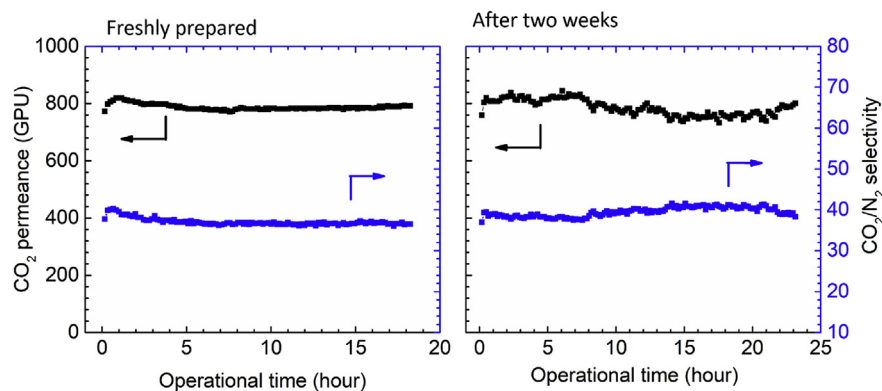


Fig. 7. Long-term stability of PVA/ProK-40 membrane.

diffusivity in general, of which the N_2 transport is more in favor than CO_2 , resulting in a compromise in the selectivity improvement. Nevertheless, the so-called “trade-off” in polymeric membranes between the permeability and selectivity has been overcome, which proves the existence of the CO_2 facilitated transport in the membranes.

Due to the high CO_2 permeance, the PVA/ProK-40 membrane was selected to investigate the long-term stability of this type of membranes. The results are shown in Fig. 7. Over the tested period, no sign of performance dropping was observed with regards to either CO_2 permeance or CO_2/N_2 selectivity. It is worth to mention that other membrane samples containing the optimal amount of amino acid salts (i.e., GlyK-30, ArgK-30, and CysK-30) were also tested following the same procedure. For each membrane, a minimum duration of 6–10 h was used for the tests to ensure the membranes being fully conditioned at the humid state and the performances being stabilized. None of the tested membranes show a noticeable reduction in either CO_2 permeance or CO_2/N_2 selectivity. In addition, after the first humid gas permeation test, the membrane module was stored for two weeks in ambient lab condition. The tested membrane module was taken for the second permeation operation without special treatment. The separation performances were found nearly unchanged in the re-test, as shown in Fig. 7. The simple storage and reliable long-term stability make the membrane promising for industrial applications.

4. Conclusion

In the present study, four different amino acid salts were employed as mobile carriers in PVA-based facilitated transport membranes for CO_2 capture. The membrane was fabricated by dip-coating the PPO substrate into 0.5 wt% polymer/amino acid salt solutions. The obtained membranes were characterized using different technics. Based on this study, some key conclusions can be made:

- (1) Defect-free, ultrathin TFC hollow fiber membranes of the PVA/amino acid salt blend with a thickness in the range of 200 nm–500 nm can be fabricated. Adding amino acid into PVA has a negligible effect on the final membrane thickness.
- (2) The thermal stability of the membranes can fulfill the post-combustion CO_2 capture requirement.
- (3) Presence of amino acid salts in the PVA matrix could remarkably improve the CO_2 permeance without sacrificing the CO_2/N_2 selectivity.
- (4) All the PVA/amino acid salts hybrid membranes exhibit good long-term stability.

The PVA/amino acid salt hybrid membranes have the potential for the industrial applications for various CO_2 separation processes considering the straightforward fabrication, promising and stable separation performance. The separation performances of these membranes

could be further improved by optimizing the polymer phase, such as employing polymers with CO_2 reactive functional groups to combine the facilitated transport effects of fixed carriers and mobile carriers.

Conflicts of interest

There are no conflicts to declare.

Acknowledgments

This work acknowledges the financial support from the European Union's Horizon 2020 Research and Innovation program under Grant Agreement No. 727734.

Appendix A. Supplementary data

Supplementary data to this article can be found online at <https://doi.org/10.1016/j.memsci.2019.02.023>.

References

- [1] M. Galizia, W.S. Chi, Z.P. Smith, T.C. Merkel, R.W. Baker, B.D. Freeman, 50th anniversary perspective: polymers and mixed matrix membranes for gas and vapor separation: a review and prospective opportunities, *Macromolecules* 50 (2017) 7809–7843.
- [2] Z. Qiao, M. Sheng, J. Wang, S. Zhao, Z. Wang, Metal-induced polymer framework membrane with high performance for CO_2 separation, *AIChE J.* 65 (2019) (2018) 239–249.
- [3] S. Rafiq, L. Deng, M.B. Hägg, Role of facilitated transport membranes and composite membranes for efficient CO_2 capture—a review, *ChemBioEng Rev.* 3 (2016) 68–85.
- [4] X.Y. Luo, X.Y. Lv, G.L. Shi, Q. Meng, H.R. Li, C.M. Wang, Designing amino-based ionic liquids for improved carbon capture: one amine binds two CO_2 , *AIChE J.* (2018) article in press.
- [5] J.D. Way, R.D. Noble, T.M. Flynn, E.D. Sloan, Liquid membrane transport: a survey, *J. Membr. Sci.* 12 (1982) 239–259.
- [6] L. Deng, M.-B. Hägg, Fabrication and evaluation of a blend facilitated transport membrane for CO_2/CH_4 separation, *Ind. Eng. Chem. Res.* 54 (2015) 11139–11150.
- [7] M. Saeed, L. Deng, CO_2 facilitated transport membrane promoted by mimic enzyme, *J. Membr. Sci.* 494 (2015) 196–204.
- [8] J. Xu, H. Wu, Z. Wang, Z. Qiao, S. Zhao, J. Wang, Recent advances on membrane-based gas separation processes for CO_2 separation, *Chin. J. Chem. Eng.* (2018) article in press.
- [9] M. Wang, Z. Wang, S. Zhao, J. Wang, S. Wang, Recent advances on mixed matrix membranes for CO_2 separation, *Chin. J. Chem. Eng.* 25 (2017) 1581–1597.
- [10] Z. Tong, W.S.W. Ho, New sterically hindered polyvinylamine membranes for CO_2 separation and capture, *J. Membr. Sci.* 543 (2017) 202–211.
- [11] Y. Liu, Z. Wang, M. Shi, N. Li, S. Zhao, J. Wang, Carbonic anhydrase inspired poly (N-vinylimidazole)/zeolite Zn- β hybrid membranes for CO_2 capture, *Chem. Commun.* 54 (2018) 7239–7242.
- [12] Y. Chen, L. Zhao, B. Wang, P. Dutta, W.S. Winston Ho, Amine-containing polymer/zeolite Y composite membranes for CO_2/N_2 separation, *J. Membr. Sci.* 497 (2016) 21–28.
- [13] Z. Dai, L. Bai, K.N. Hval, X. Zhang, S. Zhang, L.J.S.C.C. Deng, Pebax®/TSIL blend thin film composite membranes for CO_2 separation, 59 (2016) 538–546.
- [14] H.C. Ferraz, L.T. Duarte, M. Di Luccio, T.L.M. Alves, A.C. Habert, C.P. Borges, Recent achievements in facilitated transport membranes for separation processes, *Braz. J. Chem. Eng.* 24 (2007) 101–118.
- [15] Y. Gao, Z. Qiao, S. Zhao, Z. Wang, J. Wang, In situ synthesis of polymer grafted ZIFs

- and application in mixed matrix membrane for CO₂ separation, *J. Mater. Chem. A* 6 (2018) 3151–3161.
- [16] Z. Dai, L. Ansaloni, L. Deng, Recent advances in multi-layer composite polymeric membranes for CO₂ separation: a review, *Green Energy Environ.* 1 (2016) 102–128.
- [17] M.-B. Hägg, L. Deng, Membranes in gas separation, *Handbook of Membrane Separations*, CRC Press, Taylor & Francis, 2009, pp. 65–103.
- [18] Z. Tong, W.W. Ho, Facilitated transport membranes for CO₂ separation and capture, *Separ. Sci. Technol.* 52 (2017) 156–167.
- [19] J.v. Holst, G.F. Versteeg, D.W.F. Brilman, J.A. Hogendoorn, Kinetic study of CO₂ with various amino acid salts in aqueous solution, *Chem. Eng. Sci.* 64 (2009) 59–68.
- [20] J.-G. Lu, Y. Ji, H. Zhang, M.-D. Chen, CO₂ capture using activated amino acid salt solutions in a membrane contactor, *Separ. Sci. Technol.* 45 (2010) 1240–1251.
- [21] J.-G. Lu, Y.-F. Zheng, M.-D. Cheng, Membrane contactor for CO₂ absorption applying amino-acid salt solutions, *Desalination* 249 (2009) 498–502.
- [22] W.W. Ho, Membranes comprising salts of aminoacids in hydrophilic polymers, in: *Google Patents*, 1997.
- [23] L.A. El-Azzami, E.A. Grulke, Carbon dioxide separation from hydrogen and nitrogen: facilitated transport in arginine salt–chitosan membranes, *J. Membr. Sci.* 328 (2009) 15–22.
- [24] Y. Qin, J. Lv, X. Fu, R. Guo, X. Li, J. Zhang, Z. Wei, High-performance SPEEK/amino acid salt membranes for CO₂ separation, *RSC Adv.* 6 (2016) 2252–2258.
- [25] Z. Tong, W.S.W. Ho, Facilitated transport membranes for CO₂ separation and capture, *Separ. Sci. Technol.* 52 (2017) 156–167.
- [26] H.-J. Song, S. Park, H. Kim, A. Gaur, J.-W. Park, S.-J. Lee, Carbon dioxide absorption characteristics of aqueous amino acid salt solutions, *Int. J. Greenhouse Gas Contr.* 11 (2012) 64–72.
- [27] Z. Dai, H. Aboukeila, L. Ansaloni, J. Deng, M. Giacinti Baschetti, L. Deng, Nafion/PEG Hybrid Membrane for CO₂ Separation: Effect of PEG on Membrane Microstructure and Performance, *Separation and Purification Technology*, (2018) article in press.
- [28] Z. Dai, L. Ansaloni, J.J. Ryan, R.J. Spontak, L. Deng, Nafion/IL hybrid membranes with tuned nanostructure for enhanced CO₂ separation: effects of ionic liquid and water vapor, *Green Chem.* 20 (2018) 1391–1404.
- [29] I.M. Weiss, C. Muth, R. Drumm, H.O. Kirchner, Thermal decomposition of the amino acids glycine, cysteine, aspartic acid, asparagine, glutamic acid, glutamine, arginine and histidine, *BMC Biophys.* 11 (2018) 2.
- [30] Y. Cao, T.J.I. Mue.c. research, Comprehensive investigation on the thermal stability of 66 ionic liquids by thermogravimetric analysis, 53 (2014) 8651–8664.
- [31] Q. Huang, S. Bhatnagar, J.E. Remias, J.P. Selegue, K. Liu, Thermal degradation of amino acid salts in CO₂ capture, *Int. J. Greenhouse Gas Contr.* 19 (2013) 243–250.
- [32] Q. Huang, J. Thompson, L.M. Lampe, J.P. Selegue, K. Liu, Thermal degradation comparison of amino acid salts, alkanolamines and diamines in CO₂ capture, *Energy Procedia* 63 (2014) 1882–1889.
- [33] F. Kogelheide, K. Kartaschew, M. Strack, S. Baldus, N. Metzler-Nolte, M. Havenith, P. Awakowicz, K. Stapelmann, J.-W. Lackmann, FTIR spectroscopy of cysteine as a ready-to-use method for the investigation of plasma-induced chemical modifications of macromolecules, *J. Phys. Appl. Phys.* 49 (2016) 084004.
- [34] A. Barth, The infrared absorption of amino acid side chains, *Prog. Biophys. Mol. Biol.* 74 (2000) 141–173.
- [35] L. Landau, B. Levich, Dragging of a liquid by a moving plate, *Dynamics of Curved Fronts*, Elsevier, 1988, pp. 141–153.
- [36] L. Deng, T.-J. Kim, M.-B. Hägg, Facilitated transport of CO₂ in novel PVAm/PVA blend membrane, *J. Membr. Sci.* 340 (2009) 154–163.
- [37] H. Zhang, H. Tian, J. Zhang, R. Guo, X. Li, Facilitated transport membranes with an amino acid salt for highly efficient CO₂ separation, *Int. J. Greenhouse Gas Contr.* 78 (2018) 85–93.